Investigation of debonding processes in particle-filled polymer materials by acoustic emission

Part II *Acoustic emission amplitude and energy release by debonding*

R. KRAUS, W. WILKE
Abteilung Experimentelle Physik, Universität Ulm, D-89069 Ulm, Germany

A. ZHUK
Division of Applied Science, Harvard University, Cambridge, USA

I. LUZINOV, S. MINKO, A. VORONOV
Department of Physical Chemistry Institute, Ukrainian Academy of Sciences, Lviv, Ukraine

A theoretical description of the debonding process is presented by using Griffith's criterion of rupture, that is applied to the balance of free energy during the debonding of a spherical filler particle from the polymer matrix. Debonding processes in model composites prepared from epoxy and polyethylene matrix filled with glass beads of various sizes have been investigated by acoustic emission analysis. The amplitude distribution for all AE events at the debonding stress was calculated and fitted by a Weibull distribution function. By comparing the results of debonding stress with the measured amplitudes, the influence of the different filler coatings on the energy balance of debonding can be discussed on the basis of the Griffith theory.

1. Introduction

Debonding processes in particle-filled polymer composites can be described by using a model based on the Griffith theory of rupture. The change of free energy is used as a criterion for the debonding of spherical particles in a polymer matrix. Different polymer materials (epoxy, polyethylene) filled with glass beads of various sizes and surface treatment, have been investigated under tensile loading by acoustic emission analysis. The debonding stress was derived from the number of acoustic emission events per strain or stress interval. In addition, the acoustic emission technique offers the capability of measuring the amplitude of the ultrasonic stress waves, which is related to the energy release of the underlying failure mechanism [1]. The measured acoustic emission amplitude is compared to the energy of debonding, and can be derived from model calculations using the debonding stress.

2. Griffith theory of debonding

A theoretical treatment of debonding processes can be given using Griffith's [2] criterion of rupture applied to the change of free energy, ΔF

$$\Delta F = F_s - F_e < 0 \quad (1)$$

According to calculations by Gent and co-workers [3, 4] and Zhuk *et al.* [5], the change of free energy by debonding of a spherical particle from an elastic matrix is given by the difference between the surface energy, F_s, needed for the detachment of the matrix from the filler (Fig. 1).

$$F_s = S(\phi)R^2\gamma \quad (2)$$

$$S(\phi) = 2\pi(1 - \cos\phi) \quad (3)$$

(where ϕ is the debonding angle, R the particle radius, γ the surface energy (density)), and the released elastic energy, F_e

$$F_e = \frac{\sigma^2}{E}R^3W(\phi) \quad (4)$$

$$W(\phi) = \tfrac{1}{2}kq_0^2\sin^3\phi \quad (5)$$

where σ is the applied stress, E the modulus of the matrix, $W(\phi)$ the normalized mechanical energy for $R = 1$m, $\sigma = 1$ Pa, $E = 1$ Pa, k is a constant ($= 2.29$), representing the volume of stress release, and q_0 is the stress concentration factor (≈ 2)

$$\Rightarrow \Delta F = \frac{\sigma^2}{E}R^3[\bar{\gamma}S(\phi) - W(\phi)] \quad (6)$$

using

$$\bar{\gamma} = \frac{E\gamma}{\sigma^2 R} \quad (7)$$

where $\bar{\gamma}$ is the reduced surface energy.

Debonding is only possible for $\Delta F < 0$. The energy released by the debonding process, ΔW, is given by

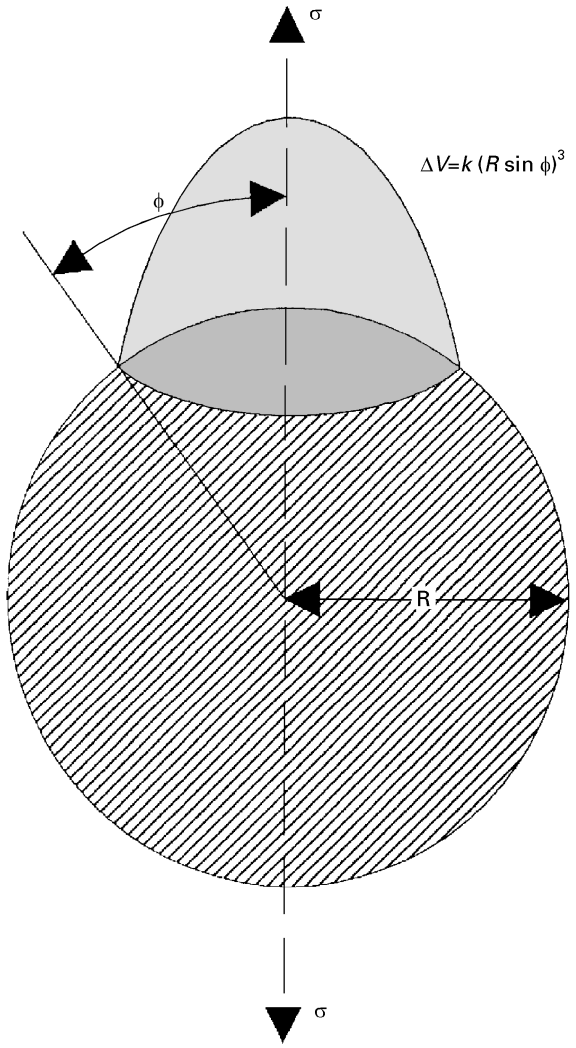

Figure 1 Model for debonding of a spherical particle from an elastic matrix under uniaxial stress, after Gent [3, 4].

the change of free energy. The initial defects (see Part I [6]) are usually small ($\phi_0 = d/R < 0.1$) and can be neglected

$$\Delta W = \underbrace{\Delta F(\phi_0)}_{\approx 0} - \Delta F(\phi) \quad (8)$$

$$= \frac{\sigma_d^2}{E} R^3 [W(\phi) - \bar{\gamma} S(\phi)] \quad (9)$$

where σ_d is the macroscopic debonding stress.

The released energy, ΔW, is primarily determined by the mechanical energy, which is reduced by the surface energy, γ, needed for the detachment of the matrix from the filler surface, especially for the case of small filler particles and large γ values. The deviation of ΔW from

$$\Delta W \propto \frac{\sigma_d^2}{E} R^3 \quad (10)$$

can be shown by plotting $\Delta W(R, \gamma)$ in double logarithmic scale (Fig. 2).

3. Experimental procedure

3.1. Materials and specimens

Two different types of model composite (epoxy resin, polyethylene) were prepared to investigate the influence of filler and matrix properties on the failure process. Experiments with composites from epoxy resin matrix filled with glass beads of various sizes (50–63, 80–90, 100–125, 160–200, 315–400 μm) and surface coatings (peroxide copolymer only, grafted layers of polystyrene or polybutylacrylate) were performed to study the effect of filler size and coating on the energy released by debonding. Another series of tests using different types of linear polyethylene matrix (medium density, trade-mark TIPELIN) with different degree of branching (Table I), filled with uncoated glass beads of various sizes, was carried out to investigate the influence of the matrix properties. A detailed description of the preparation procedures is given in Part I [6] of this paper.

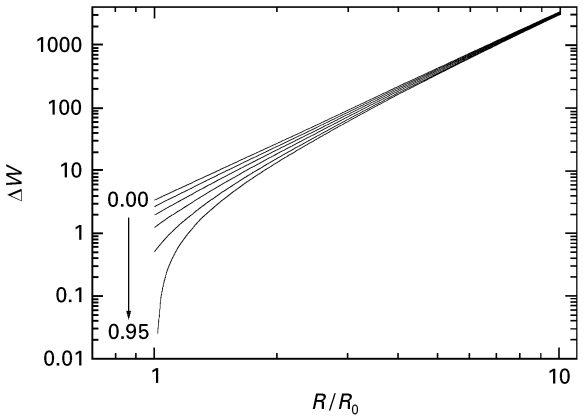

Figure 2 Normalized debonding energy depending on filler size and surface energy, $\gamma = 0$, 0.2, 0.4, 0.6, 0.8, 0.95 ($\phi = 65°$, $E = 1$ Pa, $\sigma = 1$ Pa).

3.2. Test methods

Tests were performed at constant speed. Acoustic emission was monitored on an AET Model 5500 system using a transducer with a resonant frequency of 175 kHz as described in Part I [6] of this paper. The acoustic emission amplitude, A, is calculated from the transducer signal voltage, U, as

$$A = 20 \log \frac{U}{U_{ref}} \quad (11)$$

with $U_{ref} = 0.1$ or 1 mV (40/60 dB preamplifier gain).

The type of preamplifier and the event duration clock settings were adjusted to match the dynamic range of the acoustic emission system to the individual conditions in terms of signal amplitude and event duration. For a resonant transducer, the event duration is related (approximately proportional) to the signal amplitude [1]. Therefore, low peak amplitude signals require high preamplifier gain and short clock counter intervals for maximum signal resolution, while high peak amplitude signals need low preamplifier gain and longer clock counter intervals to avoid amplifier overload and duration counter overflow.

The data were processed and analysed off-line by custom-made software in order to avoid a reduction of system performance by real-time analysis. In a first step, a device-independent file containing the values of

TABLE I Physical data of Tipelin-polyethylenes. $\bar{M}_w$ = molecular weight, weight average; $\bar{M}_n$ = molecular weight, number average; ε = degree of branching = CH_3-end groups/1000 CH_2-units; ρ = density; X_c = degree of crystallinity from WAXS or DSC; T_m = melting temperature

Tipelin type	$\bar{M}_w$	$\bar{M}_n$	ε	ρ (g cm^{-3})	X_c	T_m (°C)
BS-501-17	198 000	12 000	0.6	0.950	0.75	122
FA-470-02	187 000	20 000	2.0	0.947	0.73	119
FB-472-20			2.0	0.950	0.73	119

the variables strain, λ, stress, σ, and peak amplitude, A, was calculated from the raw AET 5500 data. These files were used to calculate frequency diagrams with respect to peak amplitude, A, and for further analysis on deformation energy using *MATLAB for Windows*. The main focus of this analysis is on the peak amplitude of the acoustic emission events near the debonding stress. Therefore, only acoustic emission events that occurred in a narrow stress interval at the debonding stress, were selected for the amplitude distributions.

For a quantitative analysis, we tried to describe the obtained amplitude distribution (histogram) by a suitable distribution function. Pollock [7] suggested several empirical distribution (e.g. Log normal) functions for amplitude distributions. Lorenzo and Hahn [8] generated amplitude distributions by computer simulation of fibre breakage in unidirectional composites, that could be fitted by a Weibull distribution function. This approach is empirical too, but has the advantage that the minimum amplitude, A_0, being determined by the sensitivity of the measurement system, can be taken into account as a fixed parameter of the distribution function [9]

$$\phi(A) = N_0 \frac{m}{A_1 - A_0}\left(\frac{A - A_0}{A_1 - A_0}\right)^{m-1} \times \exp\left[-\left(\frac{A - A_0}{A_1 - A_0}\right)^m\right] \quad (12)$$

where N_0 is the normalization parameter, A_0 the sensitivity, A_1 the amplitude parameter, and m the Weibull modulus. A formally similar and also empirical distribution function is the extreme values function used by Wu *et al.* [10]. An experimental comparison of our data with the different empirical distribution functions in question led to the result that the amplitude distributions from the deformation of the model composites are best fitted by the Weibull function. Therefore, this distribution function was fitted to the experimental amplitude distribution data by the method of a least squares fit using a Levenberg–Marquardt–Algorithm (*MicroCal ORIGIN*) to quantify the maximum of the amplitude distribution, A_{max}, near the debonding stress

$$A_{max} = A_0 + (A_1 - A_0)\left(\frac{m-1}{m}\right)^{\frac{1}{m}} \quad (13)$$

4. Results

The amplitude of an acoustic emission event correlates directly to the energy released by the underlying failure process [1]. According to the calculations in Section 2, the energy released by particle debonding, ΔW, is determined by the debonding stress and the filler size. For the following analysis we make the assumption that the debonding stress is proportional to its experimental modal value, σ_d, which was determined from the maximum of the number of acoustic emission events per stress or strain interval as described in Part I [6]. The radius, R, of the filler particles is given by the mean value of the size distribution.

4.1. Epoxy composites

Specimens of epoxy composites filled with glass beads with different polymer coatings and of various size, have been investigated by tensile loading until rupture at room temperature ($T = 22$ °C). The influence of the polymer coatings on the measured acoustic emission amplitude is comparatively small, but it depends strongly on the filler size [11] as it is shown in Table II. For most filler sizes, the peak amplitude is maximum for samples only with a coating of peroxide copolymer, but there is no clear ranking between the different coatings. An example for an experimental amplitude distribution with fitted Weibull distribution function is presented in Fig. 3. The errors given for the fitted parameters and modal values of peak amplitude were derived from the standard deviations (square root of Weibull variances). The parameter A_0 (lower bound for amplitude) is not fitted, but determined by the settings of the acoustic emission detector.

TABLE II Peak amplitude: epoxy composites

Coating	Filler size $2R$ (μm)	Amplitude, A_{max} (dB)
Peroxide copolymer	50–63	45 ± 1
	100–125	62 ± 1
	160–200	77 ± 1
	315–400	82 ± 5
Polybutylacrylate (additional)	50–63	37 ± 1
	80–90	51 ± 1
	100–125	66 ± 2
	160–200	70 ± 3
Polystyrene (additional)	50–63	36 ± 1
	100–125	59 ± 1
	160–200	75 ± 2
	315–400	94 ± 2

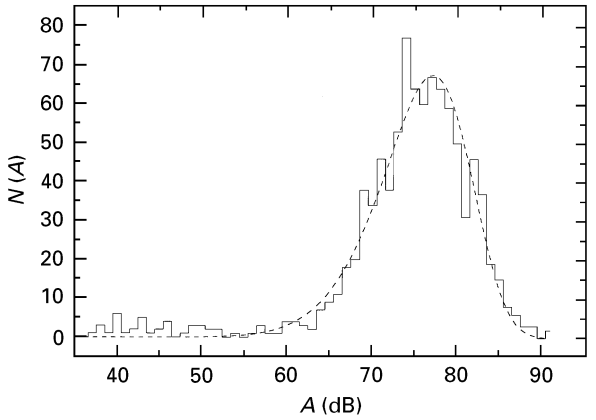

Figure 3 Amplitude distribution for epoxy composite with 160–250 μm glass beads coated with peroxide copolymer only, with a fitted Weibull distribution function. $N_0 = 902 \pm 40$, $A_0 = 35.0$, $A_1 = 77.7 \pm 0.27$, $m = 8.63 \pm 0.45$.

TABLE III Peak amplitude: polyethylene composites

Matrix type	Filler size $2R$ (μm)	Amplitude, A_{max} (dB)
BS-501-17	80–110	40 ± 1
	160–250	60 ± 1.5
	290–420	76 ± 1.5
FA-470-02	80–110	30 ± 1.5
	160–250	46 ± 1
	290–420	70 ± 2
FB-472-20	80–110	29 ± 1.5
	160–250	48.5 ± 1
	290–420	71 ± 1

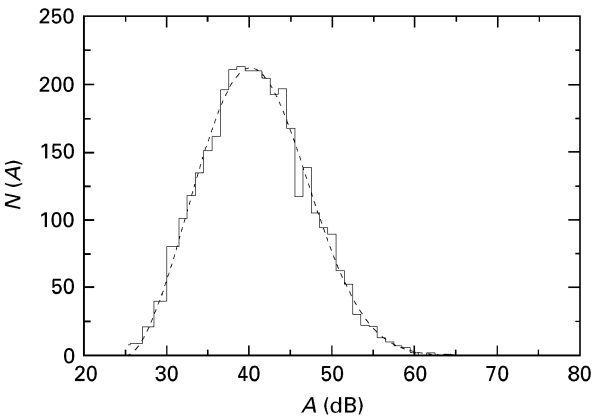

Figure 4 Amplitude distribution for polyethylene composite BS-501-17 with 80–110 μm glass beads with a fitted Weibull distribution function. $N_0 = 3.45 \times 10^3 \pm 44$, $A_0 = 2.50$, $A_1 = 42.8 \pm 0.11$, $m = 2.76 \pm 0.041$.

4.2. Polyethylene composites

Specimens of polyethylene composites filled with glass beads of various sizes have been investigated by tensile loading at room temperature ($T = 22\,^{\circ}\mathrm{C}$). Three groups of composites with matrices of ethylene–hexene–copolymers with different degree of branching and density were tested. The influence of the different polymer matrices on the measured acoustic emission amplitude is comparatively small, but it depends strongly on the filler size, as shown in Table III. Overall there is a marked difference mainly between the samples made from BS-501-17 (low degree of branching) on one side and the samples made from FA-470-02 and FB-472-20 (higher degree of branching) on the other side. The samples with BS-501-17 matrix show higher amplitude values at the debonding stress than the other samples for all filler sizes.

Fig. 4 shows, as an example, the experimental amplitude distribution with fitted Weibull distribution function for BS-501-17 matrix filled with glass beads of 80–110 μm diameter. The errors given in the table and in the diagram were derived from Weibull variances as described above.

5. Discussion

According to the calculations in Section 2, the energy released by particle debonding, ΔW, is given by

$$\Delta W = \frac{\sigma_d^2}{E} R^3 [W(\phi) - \bar{\gamma} S(\phi)] \tag{14}$$

If we neglect the influence of the reduced surface energy, $\bar{\gamma}$, and the debonding angle, ϕ, the released energy, ΔW, should be proportional to the macroscopic deformation energy, W_d, at the debonding stress, σ_d. As the deformation of the composites is not strictly elastic, W_d is calculated by numerical integration of $\sigma(\lambda)$

$$\Delta W \propto \frac{\sigma_d^2}{E} R^3$$

$$\propto W_d \tag{15}$$

$$W_d = \int_{\lambda=1}^{\lambda_d} \sigma(\lambda)\, d\lambda\, R^3 \tag{16}$$

Wolters [1] showed that, in the case of fibre breakage, the acoustic emission signal voltage, U, is proportional to the released energy. The signal voltage, U, is directly measured by the transducer and related to the peak amplitude by

$$A = 20 \log\left(\frac{U}{U_{ref}}\right) \tag{17}$$

where A_0 is the apparatus constant. Now, we assume that this is also true for debonding in a particulate composite. Thus, the acoustic emission signal voltage, U, should also be proportional to the deformation energy, W_d

$$U_{max} \propto W_d \tag{18}$$

$$\rightarrow A = A_0 + 20 \log\left(\frac{W_d}{W_0}\right) \tag{19}$$

where W_0 is the normalization constant. Differences in debonding energy because of different values of surface energy and debonding angle should be noticeable as deviations from the linear plot $A(\log W_d)$.

5.1. Epoxy composites

The results of the experiments with epoxy composites agree very well with these predictions. Plotted against

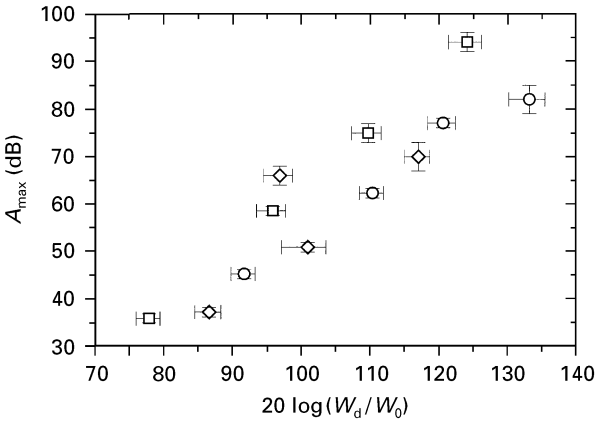

Figure 5 Correlation between acoustic emission amplitude and calculated debonding energy for epoxy composites filled with glass beads with different coatings and various sizes. (○) Peroxide copolymer only, (◇) polybutylacrylate, (□) polystyrene.

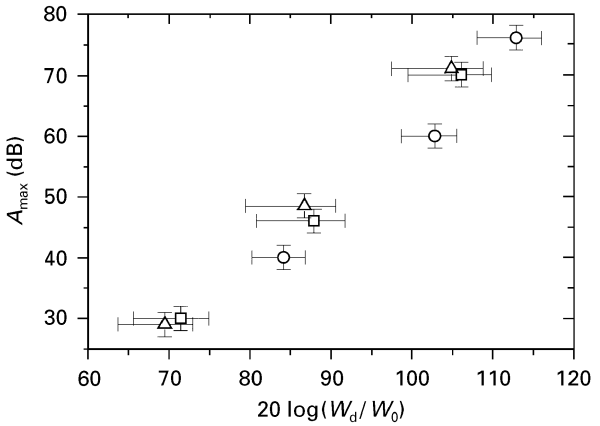

Figure 6 Correlation between acoustic emission amplitude and calculated debonding energy for polyethylene composites filled with glass beads of various sizes. (○) BS-501-17, (□) FA-470-02, (△) FB-472-20.

$\log(W_d)$, the amplitude values for all samples with the same filler coating show a linear behaviour with only a few exceptions. As shown by the diagram in Fig. 5 it is remarkable that, for samples coated with polystyrene, all amplitude values are higher than the corresponding data points for the other samples.

According to our theory, these differences should be determined by the expression $[W(\phi) - \bar{\gamma}S(\phi)]$, i.e. by the surface energy and the debonding angle, which are also related to the debonding stress. The analysis of the debonding stress is described in Part I [6]. The results for σ_d indicate that, for samples with polystyrene coating, $\bar{\gamma}$ is reduced and therefore the energy released by acoustic emission is higher, compared to the deformation energy, W_d. This correlation between comparatively high AE amplitude and low debonding stress is characteristic for all epoxy samples. Obviously, the low debonding stress, which indicates poor adhesion between filler and matrix, is the reason for comparatively high acoustic emission amplitudes. From the perspective of the Griffith theory, this means that a smaller fraction of the mechanical energy, which is released by the debonding process, is dissipated by the formation of new surfaces, and therefore a greater fraction can be detected as acoustic emission.

Compared to those specimens, where the filler particles are coated only with peroxide copolymer, the samples coated with polybutylacrylate show only slightly smaller AE amplitudes, but a strong decrease in debonding stress. In our model the energy released by debonding is mainly determined by the adhesion (corresponding to debonding stress) and the stress concentration by the filler particle. Therefore, the results for polybutylacrylate, indicate that the soft layer of polybutylacrylate reduces the adhesion and stress concentration as well. An overview of the results is given in Fig. 5. The error bars represent the estimated error for W_d, including the errors of σ_d and λ_d (x-axis) and the error derived from Weibull variances for A_{max} (y-axis).

5.2. Polyethylene composites

The experimental data for the polyethylene composites were evaluated in the same way. In this case, too, a linear correlation between the acoustic emission amplitude and the logarithm of the deformation energy at the stress of debonding is noticeable. The debonding stress data are given in Part I [6]. The samples with the highest debonding stress (matrix BS-501-17, low degree of branching) exhibit (compared to the deformation energy) the lowest AE amplitude. The other composites (matrix FA-470-02 and FB-472-20) show only slight differences in debonding stress and also in peak amplitude. In all, the ranking of the curves A_{max} ($\log W_d$) follows the order of the modal values for debonding stress, as shown in Fig. 6. The error bars were determined as described above.

6. Conclusion

A theoretical description of the debonding process is presented using Griffith's criterion of rupture, that is applied to the balance of free energy during the debonding of a spherical filler particle from the polymer matrix.

Debonding processes in model composites prepared from epoxy and polyethylene matrices filled with glass beads of various sizes, have been investigated by acoustic emission analysis. Each debonding event is detected as one distinct acoustic emission event, whose amplitude is measured. The amplitude distribution (histogram) for all AE events at the stress of debonding was calculated. Then a Weibull distribution function was fitted to the experimental data to determine the maximum of the amplitude distribution.

Comparing the results for debonding stress with the measured AE amplitudes, it is possible to estimate the influence of the different filler coatings on the energy balance of debonding. The elastic energy which is released by debonding and induces acoustic emission, is determined by the deformation energy at the debonding stress. Depending on the surface energy which is dissipated by the detachment of the matrix from the filler surface, the amount of energy released as acoustic emission is (compared to the deformation energy) lower for filler particles with high debonding stress, i.e. surface energy.

Acknowledgements

We are grateful for the support of the Deutsche Forschungsgemeinschaft (DFG). The collaboration between the groups from Ulm (Germany) and Lviv (Ukraine) was supported by the NATO Scientific Affairs Division under HTECH.LG.940579.

References

1. J. WOLTERS, "Anwendung der Schallemissions-Meßtechnik zum Beschreiben von Versagensmechanismen in partikelgefüllten Thermoplasten", Fortschr.-Ber. VDI Reihe 5 Nr. 163, VDI Verlag, Düsseldorf (1989).
2. A. A. GRIFFITH, *Trans. R. Soc. Lond.* **A221** (1920) 163.
3. A. N. GENT, *J. Mater. Sci.* **15** (1980) 2884.
4. A. N. GENT and BYOUNGKYEU PARK, *ibid.* **19** (1984) 1947.
5. A. V. ZHUK, V. G. KNUNYANTS, V. G. OSHMYAN and V. A. TOPOLKARAEV, *ibid.* **28** (1993) 4595.
6. R. KRAUSS, W. WILKE, A. ZHUK, I. LUZINOV, S. MINKO and A. VORONOV, *ibid.* **32** (1997).
7. A. A. POLLOCK, "International Advances in Nondestructive Testing", Vol. 7, Gordon and Breach Science, (1981) pp. 215–39.
8. L. LORENZO, H. T. HAHN, *J. Acoust. Emission* **5** (1986) 15.
9. W. WEIBULL, *J. Appl. Mech.* **18** (1951) 293.
10. Y. H. WU, M. H. YANG, J. Y. KUO and S. P. CHANG, in "SPI International Symposium Acoustic Emission from Reinforced Composites", edited by G. C. Sih and S. E. Hsu, Vol. 2, Montreal (VNU Science, Utrecht, 1987).
11. R. KRAUS, A. ZHUK, I. LUZINOV, S. MINKO and W. WILKE, in "ECCM CTS2 2nd European Conference on Composite Materials, Composite Testing and Standardisation", edited by P. J. Hogg, K. Schulto and H. Wittach, Hamburg (Woodhead, Cambridge, 1994).

Received 23 February 1996
and accepted 10 February 1997